frontiers | Frontiers in Mechanical Engineering

TYPE Original Research
PUBLISHED 16 December 2025
DOI 10.3389/fmech.2025.1736852

OPEN ACCESS

EDITED BY
Hongsheng Guo,
National Research Council Canada (NRC), Canada

REVIEWED BY
Jinlong Liu,
Zhejiang University, China
Reza Farzam,
Simon Fraser University, Canada

*CORRESPONDENCE
Yue Wu,
wuuy0901@outlook.com

RECEIVED 05 November 2025
REVISED 27 November 2025
ACCEPTED 28 November 2025
PUBLISHED 16 December 2025

CITATION
Wu Y and Qiu T (2025) The influence of diesel pilot injection timing on the combustion and emission characteristics of a natural gas-diesel dual-fuel engine.
Front. Mech. Eng. 11:1736852.
doi: 10.3389/fmech.2025.1736852

The influence of diesel pilot injection timing on the combustion and emission characteristics of a natural gas-diesel dual-fuel engine

Yue Wu* and Tao Qiu

College of Mechanical and Energy Engineering, Beijing University of Technology, Beijing, China

This study investigated the effects of varying diesel pilot injection timings (19°–25° BTDC) on the thermal efficiency, combustion, and emission characteristics of an engine operating under different load ranges (25%–100%) using a modified single-cylinder natural gas-diesel dual-fuel (NDDF) engine. The results indicate that advancing the injection timing can significantly improve brake thermal efficiency (BTE) under partial loads (25%–75%), but efficiency decreases at 100% load. Specifically, advancing the timing to 25° BTDC results in a reduction in BTE compared to 23° BTDC. This suggests that the negative compression work generated by excessively early combustion exceeds the benefits from improved combustion, thereby establishing a physical limit for advanced injection under high-load conditions. Combustion analysis identified a distinct "combustion phase shift" phenomenon. The results show that although advanced injection shifts the combustion phase closer to the favorable high-temperature region near top dead center (TDC), there is only a slight change in combustion duration. This is mechanically attributed to the over-leaning of the pilot diesel spray during prolonged ignition delay. The consequent formation of weak combustion cores slows initial flame propagation, counteracting the accelerating effects of improved thermodynamics. Emission analysis reveals a trade-off: advanced injection reduces smoke emissions by up to 4.2% but substantially increases nitrogen oxides (NOx). Concurrent increases in carbon monoxide (CO) with advanced timing suggest local quenching and over-leaning effects. Additionally, a dynamic fuel substitution strategy was employed to optimize the NDDF engine, successfully maintaining efficiency while mitigating detonation. This study provides a validated experimental basis for the precise calibration of dual-fuel engines across the load range.

KEYWORDS

brake thermal efficiency, diesel, dual-fuel engine, emissions, NATURAL GAS, pilot injection timing

1 Introduction

In recent years, the exhaust emissions of diesel engines, particularly nitrogen oxides (NOx) and particulate matter (PM), have drawn significant concern. Against this backdrop, natural gas-diesel dual-fuel (NDDF) technology has attracted growing interest as a viable approach to mitigate these issues (Guo et al., 2018a). The NDDF engine operates primarily on natural gas, with diesel fuel serving as an ignition source. This combustion strategy

retains the typical diesel engine characteristics of high compression ratio and high thermal efficiency, while simultaneously reducing harmful emissions (Jamrozik et al., 2019). However, challenges such as combustion instability and elevated emissions of unburned hydrocarbons (HC) and carbon monoxide (CO) remain obstacles to its broader adoption (López et al., 2009; Ryu, 2013). In NDDF engines, the ignition process is governed mainly by the injected diesel fuel. Given that natural gas has a high auto-ignition temperature (around 650 °C), it does not readily undergo auto-ignition under in-cylinder conditions at the end of the compression stroke. The injected diesel forms localized fuel-rich zones, which auto-ignite due to compression heating and subsequently ignite the surrounding premixed natural gas–air mixture (Panoutsou et al., 2021). The ignition delay of dual-fuel engines is typically longer than that in pure diesel mode, primarily because the presence of natural gas alters the chemical and thermodynamic environment within the cylinder. The introduction of natural gas reduces the oxygen concentration and absorbs part of the compression heat, which makes the self-ignition conditions of diesel more severe (Wang et al., 2021).

To overcome these obstacles, previous studies have proposed strategies that focus on optimizing diesel injection parameters -specifically, advancing injection timing or increasing injection pressure -to improve engine ignition characteristics at low loads (Tripathi and Dhar, 2022; Akbarian et al., 2018). Diesel injection timing is a crucial variable that significantly influences the combustion and emission characteristics of dual-fuel engines. It determines the atomization and mixing of diesel, as well as the subsequent combustion of natural gas (Namasivayam et al., 2010). Guo et al. conducted a comparative study on the combustion characteristics and emissions of heavy-duty engines when operating in pure diesel mode and NDDF mode at low loads. The result shows that under low-load conditions, advancing the start of injection (SOI) in NDDF mode outperforms traditional diesel combustion by effectively boosting thermal efficiency while mitigating methane (CH4) and total greenhouse gas (GHG) emissions. (Guo et al., 2018b). Amin et al. corroborate the GHG benefits of advanced timing at low loads, while noting that for medium-to-high loads, emission abatement is more effectively achieved by increasing the natural gas fraction. (Yousefi et al., 2020). Dai and Jia et al. further clarified the mechanism of advanced injection through numerical simulation. They observed that when the injection timing was 17° BTDC, the diesel spray formed a distributed ignition pattern within the cylinder. In this case, the flame propagation speed was 40% higher than that at 5° BTDC, reaching 2.5 m/s (Dai et al., 2020). Van et al. found through numerical simulation that premature injection can prolong the evaporation time, which facilitates thorough mixing with air. However, this process is prone to being affected by the uneven temperature distribution inside the cylinder. On the contrary, excessively slow injection can cause diesel to accumulate on the cylinder wall or in high-temperature areas, thereby forming local oil-rich zones (P et al., 2021). In the numerical simulation study by Pavlos et al., advancing the injection timing to 17° BTDC resulted in a 30% increase in the volume of the combustible mixture area formed by the diesel spray during the compression stroke, and a 15% increase in flame propagation speed. This ensures the complete combustion of natural gas during the expansion process (Dimitriou et al., 2020). In the research of Zhang et al., it was proposed that the pilot diesel injection timing (PDIT) directly affects the ignition delay period and plays a key role in the thorough mixing of natural gas and air in the cylinder. Either excessively advanced or retarded PDIT results in low thermal efficiency during the cycle. Therefore, an improper PDIT fails to ensure efficient combustion, thereby affecting the engine's operating performance (Zhang et al., 2024). Wang et al. studied pilot diesel ignition modes and the combustion and emission characteristics under low load conditions. The results showed that with the advancement of diesel injection timing, brake thermal efficiency (BTE) and total hydrocarbon (THC) emissions remained almost unchanged, while NOx emissions decreased significantly. However, due to the low temperature inside the cylinder, excessively early injection will inevitably lead to diesel wall impact and worsen atomization quality (Wang et al., 2016). Research by Jie Liu et al. indicated that advancing the pilot fuel injection timing under high-load conditions resulted in increased NOx emissions (Liu et al., 2013). Tripathi et al.'s research indicates that advancing the pilot injection timing to 24° BTDC reduces methane slip, HC, and CO emissions. However, when the pilot injection timing is advanced beyond 24° BTDC, the emissions of methane slip, HC, and CO all increase (Tripathi et al., 2022).

Although the influence of injection timing in dual-fuel engines has been widely studied, further experimental verification is still required to precisely balance ignition delay, flame propagation, and emission generation under varying loads and substitution rates. Furthermore, observations regarding how injection timing affects combustion and emissions vary across different engine configurations, and a consensus has yet to be reached. Therefore, a profound understanding of the mechanisms by which diesel injection timing influences combustion paths, thermal efficiency, and pollutant generation is crucial for optimizing the performance of dual-fuel engines. Against this background, this study established a diesel-compressed NDDF combustion system based on a modified single-cylinder diesel engine to investigate the influence of pilot injection timing on combustion and emission characteristics.

1.1 Engine set up

This study was conducted on a modified naturally aspirated single-cylinder direct-injection diesel engine, and its engine parameters are listed in Table 1. The dual-fuel supply system consisted of an additional natural gas supply system based on the original diesel engine supply system, and ignition was achieved through the traditional diesel ignition injection system using compression ignition. Diesel fuel was supplied by an electronic pump unit and directly injected into the cylinder through the diesel injector. The natural gas supply system consisted of a CNG storage tank, a pressure reducer, a natural gas flow meter, and a natural gas rail. After being regulated to low pressure by a pressure reducer, the natural gas was injected into the intake manifold through a natural gas injector connected to a hose. A throttle valve was installed on the main intake pipe to control the engine's intake volume, thereby achieving precise regulation of the excess air coefficient. The electronic control unit (ECU) collected engine signals such as engine speed, temperature, and intake pressure, and controlled the intake flow and fuel injection through duty ratio adjustment.

An ASAIR-AMC2100 air flow meter was installed upstream of the throttle valve to measure the intake air flow. Another ASAIR-AMC2100 flow meter was installed upstream of the CNG rail to measure the CNG flow. A DIN-835 burette meter was installed downstream of the diesel fuel tank for measuring diesel consumption. Additionally, a KISTLER-6052C piezoelectric pressure sensor was installed inside the cylinder head to collect in-cylinder pressure data. The engine load was measured using an ET4000 electric dynamometer. A TMR combustion analyzer was used, which was equipped with functions for analyzing the combustion process, collecting data, processing data, and analyzing data. The engine's smoke opacity and gaseous emissions (including carbon monoxide (CO), carbon dioxide (CO_2), hydrocarbons (HC), and nitrogen oxides (NO_x)) were measured using a GZFULI-FLB-100 opacity smoke meter and a VARIOplus-new exhaust gas analyzer, respectively. The engine setup is shown in Figure 1. The specifications and parameters of the main instruments used in this study are presented in Table 2. The properties of fuels are shown in Table 3.

TABLE 1 Engine specifications.

Items	Specifications
Type	Four-stroke direct-injection single-cylinder diesel engine
Rated power	8.1 kW
Rated speed	3000RPM
Bore × stroke	92 × 75 mm
Displacement	498cc
Injection pressure	120 MPa
Compression ratio	18

1.2 Experimental conditions and procedure

To investigate the influence of diesel injection timing on brake thermal efficiency under combined variations in engine load and CNG substitution rate, the experiments were conducted at 25%, 50%, 75%, and 100% of full load, with corresponding diesel injection timings set at 19°, 21°, 23°, and 25°BTDC, respectively. Under each of these operating conditions, the CNG mass flow rate was varied at 0, 0.2, 0.4, 0.6, and 0.8 kg/h. Where a CNG flow rate of zero corresponds to pure diesel operation. In the tests, the engine speed was maintained at its rated value of 3,000 rpm, and the global equivalence ratio (λ) was constant at 1.4. In the experiment, the effect of the various conditions mentioned above on the brake thermal efficiency of the engine was investigated.

In subsequent experiments, the engine speed was maintained at 1700 rpm, and the load was set at 75% of full load using a dynamometer, to investigate the impact of polit diesel injection timing on the performance and exhaust emission characteristics of the NDDF engine. In the experiment, the diesel injection pressure was maintained at a constant 120 MPa, and the injection duration was fixed at 280 μs per cycle. The mass flow rates of intake air, diesel fuel, and CNG were measured using an air flow meter, a diesel burette, and a CNG flow meter. The corresponding values are 30.5 kg/h, 0.55 kg/h, and 0.6 kg/h, respectively. Based on these flow rates, the energy substitution ratio (ESR) of natural gas to diesel was calculated to be 1.35. In-cylinder pressure data were obtained by using a Kistler 6052C pressure transducer with a Kistler 5018A charge amplifier. An Omron E6B2-CWZ61X encoder provided crank angle resolution. A custom LabVIEW-based control system synchronized collected pressure with the encoder signal and captures 200 consecutive engine cycles at a sampling resolution of 5 points per crank angle (°CA). The final in-cylinder pressure was calculated by averaging the data from these 200 cycles to minimize variability between cycles.

To eliminate the electrical noise interference in the encoder signal, the Wayjun-DIN33-IBF-S5-P1-O3 model signal isolation transmitter was used. This device can isolate, collect, and convert differential signals, converting encoder signals with interference into 5V level signals, thereby ensuring higher-precision crankshaft angle values to achieve precise pressure phase control.

The heat release rate is determined via the first law of thermodynamics and is expressed by (Willems et al., 2021),

$$HRR = \frac{\gamma}{1-\gamma}\, p \cdot \frac{dV}{d\varphi} + \frac{1}{1-\gamma}\, V \cdot \frac{dp}{d\varphi}$$

Where HRR represents the heat release rate, γ is the adiabatic coefficient of the in-cylinder working medium, p denotes the collected in-cylinder pressure, φ is the crank angle, and V represents the in-cylinder volume at the current crank angle. The internal volume V of the cylinder can be calculated using the following formula:

$$V = Vc + \frac{\pi D^2}{4} r \left[(1 - \cos\varphi) + \frac{\lambda}{4} (1 - 2\cos 2\varphi) \right]$$

Where Vc represents the cylinder volume at top dead center, D represents the cylinder diameter, r represents the crank radius, and λ is the ratio of the crank radius to the connecting rod length. The ignition delay time is determined by the cylinder pressure derivative threshold method (Katrašnik et al., 2006). The cylinder pressure signal was first filtered to reduce noise, and the first derivative of pressure with respect to crank angle, $dp/d\theta$, was then computed. The start of combustion, denoted as t_{ign}, was defined as the crank angle position at which the pressure derivative first reaches 10% of its maximum value, as shown in the formula below,

$$\tau_{ID} = t_{ign} - t_0$$

$$t_{ign} = min\left\{ t \left| \frac{dp}{d\theta}(\theta) \geq 0.1 \left(\frac{dp}{d\theta} \right)_{max} \right. \right\}$$

Where, τ_{ID} represents the time of ignition delay, t_{ign} represents the start moment of combustion, t_0 is the start moment of fuel injection, and $(dp/d\theta)max$ is the maximum value of the pressure derivative.

To study the influence of diesel injection timing on emissions under different engine loads, the engine speed was maintained at a constant 1700 rpm, and the diesel fuel flow rate was controlled at a fixed value of 0.7 kg/h. The engine load was controlled by adjusting the CNG flow rate, with the throttle remaining fully open during the experiments. The engine load was set to 25%, 50%, 75%, and 100%,

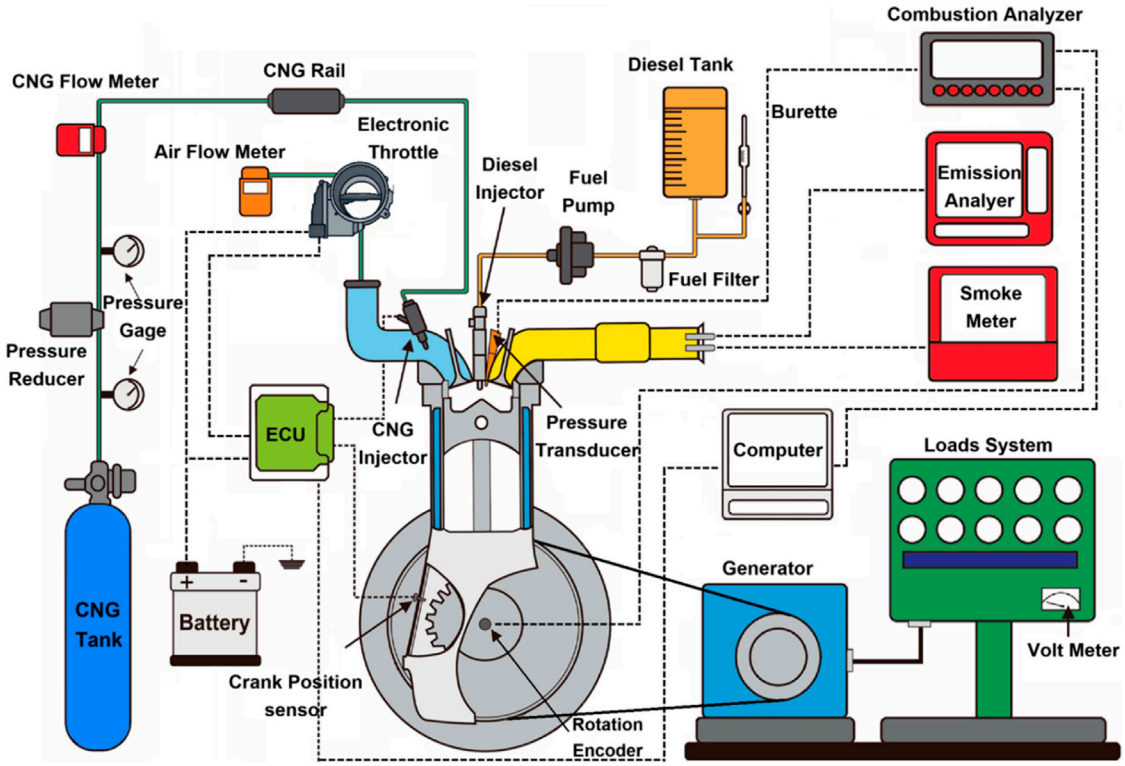

FIGURE 1
Experimental CNG-Diesel Dual fuel Engine system setup.

TABLE 2 Equipment specifications.

Instrument	Specifications	Range	Precision	Uncertainty (%)
Dynamometer	Engine speed	0–10000 r/min	±1r/min	0.03
	Torque	0-500Nm	±0.25Nm	0.05
Burette	Diesel fuel flow rate	1–30 cc	±0.2 cc	0.75
Pressure transducer	In cylinder pressure	0–250 bar	±0.1 bar	0.04
Mass flow meter	CNG flow rate	5 L/min	±1%	1.12
Exhaust analyzer	NOx emission	5,000 ppm	±10 ppm	1.4
	CO emission	0–30000 ppm	±30 ppm	1.12
	CO2 emission	0%–50%	±0.5%	0.56
	HC emission	0–10000 ppm	±30 ppm	3.35
	Smoke	0%–99% (opacity)	±0.1%	0.11

and the excess air ratio (λ) varied to 2.9, 2.3, 1.8, and 1.4, respectively. The CNG flow rates corresponding to these load conditions were 0.2 kg/h, 0.4 kg/h, 0.6 kg/h, and 0.7 kg/h, respectively.

1.3 Uncertainty analysis

The total uncertainty, U_R, of the experimental results was determined by combining the systematic uncertainty, B_R, and the random uncertainty, P_R. This is accomplished through the root-sum-of-squares (RSS) method, which is a widely adopted approach in engineering experiments for uncertainty propagation. The mathematical expression of the RSS method is given as Eq (Coleman et al., 1989),

$$U_R = \left(B_R^2 + P_R^2\right)^{1/2}$$

The general uncertainty analysis expression, respectively, gives the system uncertainty B_R and random uncertainty P_R,

TABLE 3 Properties of fuels.

Item	Diesel	Item	CNG
Flash point (PM, ˚C)	72	Ignition temperature (˚C)	580
Kinematic viscosity (20 ˚C, mm²/s)	2.73	Specific gravity (compared to air)	0.55
Density (20 ˚C, kg/m³)	826	Burning range (%)	5–15
Low heating values (MJ/kg)	43.7	Low heating value (MJ/kg)	54.1
Sulfur (mg/kg)	8.5	Methane (Vol.%)	85.13
Cetane index	51.5	Ethane (Vol.%)	9.35
Content of C (%)	84.14	Propane (Vol.%)	0.58
Content of H (%)	14.6	i-butane (Vol.%)	0.55
Content of O (%)	0.26	n-butane (Vol.%)	0.42
		Nitrogen (Vol.%)	0.01

$$\frac{B_R}{R} = \left[\sum_{i=1}^{n}\left(\frac{1}{R}\frac{\alpha R}{\alpha X_i}B_i\right)^2\right]^{1/2}$$

$$\frac{P_R}{R} = \left[\sum_{i=1}^{n}\left(\frac{1}{R}\frac{\alpha R}{\alpha X_i}P_i\right)^2\right]^{1/2}$$

In the equation, where R is a physical parameter that depends on each variable X_i. P_R and P_i, respectively, represent the uncertainty and measurement level of R.

Table 2 lists the instruments used in this study and their corresponding uncertainties. Based on the uncertainty propagation analysis, the maximum relative system uncertainty of braking thermal efficiency is determined to be 1.12%. Within the range of variations in operating conditions, the overall relative system uncertainty is between 0.75% and 1.12%.

To further reduce the impact of random errors and improve the reliability of the results, all experimental conditions underwent three repeated steady-state tests. The values reported are the arithmetic mean of these repeated tests. This method enhances the validity of conclusions drawn from the experimental data.

2 Results and discussion

2.1 Brake thermal efficiency

Figures 2–5 present the variations in BTE for CNG flow rates of 0.2, 0.4, 0.6, and 0.8 kg/h, respectively. These tests were conducted under load conditions of 25%, 50%, 75%, and 100%, with injection timings (IT) set at 19˚, 21˚, 23˚, and 25˚ BTDC. The diesel flow rate of corresponding conditions are shown in Table 4. It can be observed that as the load increases, the brake thermal efficiency corresponding to each injection timing increases and reaches its maximum value at 100% load. This indicates that when the engine operates under high load, both fuel utilization rate and mechanical efficiency improve. Meanwhile, the growth rate of effective work exceeds that of heat loss. Therefore, the engine exhibits higher brake thermal efficiency under high load conditions.

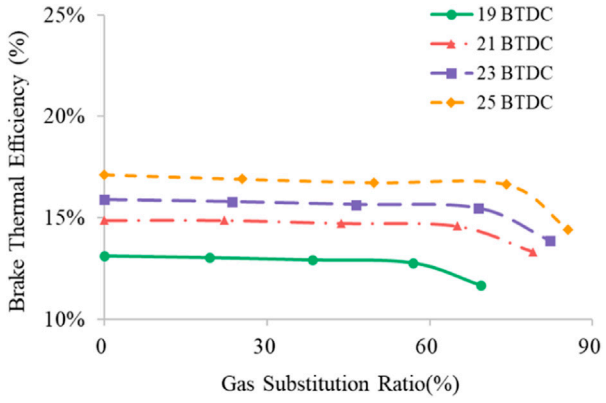

FIGURE 2
Variation of BTE with GSR at different IT under 25% Load.

Under the same load condition, the brake thermal efficiency corresponding to each injection timing first increases and then decreases with the increase of CNG flow rate, reaching its maximum at 0.6 kg/h. At a relatively low CNG flow rate, the lean mixture of compressed natural gas and air is not conducive to the formation of auto-ignition centers, which in turn leads to incomplete combustion and a subsequent decrease in brake thermal efficiency. However, at a relatively high CNG flow rate (0.8 kg/h), the higher CNG flow rate will lower the initial combustion temperature inside the cylinder. In addition, the high-concentration CNG during the compression stroke can also induce knock factors. Therefore, the brake thermal efficiency decreases again.

As can be seen from Figures 2–4, under a load of 25%–75%, the brake thermal efficiency shows an overall increasing trend as the timing advances from 19˚ BTDC to 25˚ BTDC. Among these, under the condition of a CNG flow rate of 0.6 kg/h, this adjustment led to increases of 3.86%, 3.72%, and 4.48% in BTE, respectively. This is because advancing the injection causes the diesel fuel to undergo a longer physical delay at a lower temperature, resulting in better air-fuel mixing and the formation of a more homogeneous mixture. Consequently, more uniformly distributed ignition cores are

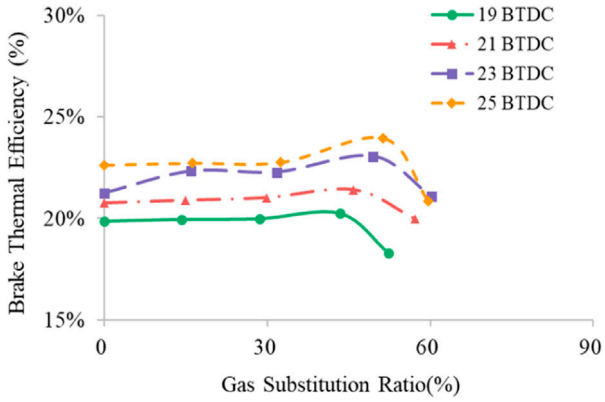

FIGURE 3
Variation of BTE with GSR at different IT under 50% Load.

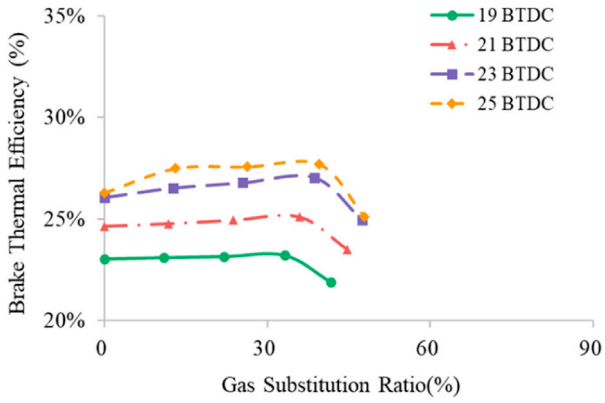

FIGURE 4
Variation of BTE with GSR at different IT under 75% Load.

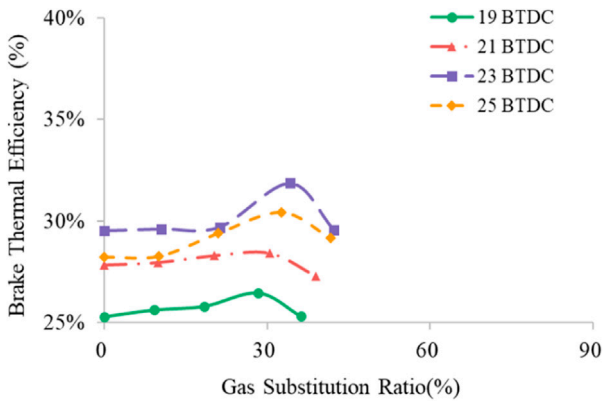

FIGURE 5
Variation of BTE with GSR at different IT under 100% Load.

TABLE 4 Diesel flow rate of corresponding conditions (kg/h).

CFR (kg/h) IT° (BTDC)		0.00	0.20	0.40	0.60	0.80
25% load	19°	1.27	1.03	0.80	0.56	0.44
	21°	1.12	0.87	0.64	0.40	0.26
	23°	1.05	0.80	0.57	0.34	0.21
	25°	0.97	0.73	0.50	0.26	0.17
50% load	19°	1.68	1.43	1.19	0.93	0.87
	21°	1.61	1.36	1.11	0.84	0.72
	23°	1.57	1.26	1.02	0.73	0.63
	25°	1.48	1.23	0.99	0.68	0.65
75% load	19°	2.17	1.93	1.69	1.44	1.33
	21°	2.03	1.78	1.53	1.28	1.18
	23°	1.92	1.65	1.39	1.14	1.05
	25°	1.90	1.58	1.34	1.09	1.04
100% load	19°	2.64	2.37	2.11	1.81	1.68
	21°	2.40	2.15	1.88	1.63	1.49
	23°	2.26	2.02	1.77	1.38	1.30
	25°	2.36	2.12	1.79	1.48	1.33

formed, and the premixed combustion speed is increased (Zhou et al., 2019). Therefore, the improved combustion quality leads to an increase in BTE.

This increase can also be observed in Figure 5, but the BTE of 25° BTDC decreased by 1.46% compared with that of 23° BTDC. The reason for this is that when the engine operates under high load, the mixture concentration in the engine cylinder is high, and the initial temperature and pressure ratio are also high. As a result, the combustion rate itself is relatively fast, which is reflected in a short ignition delay period and concentrated heat release. However, if the injection timing is advanced excessively, it may cause the combustion process to advance too early into the compression stroke. The pressure generated by combustion will then consume additional piston compression work; the negative compression work caused by excessively early injection outweighs the benefits of improved combustion, leading to a decrease in the overall BTE.

2.2 Combustion characteristics

Figure 6 shows the in-cylinder pressure changes of the diesel-compressed natural gas dual-fuel engine at injection timings of 19°, 21°, 23° and 25° BTDC. The curves in the figure exhibit a trend of increasing slowly first, then rising sharply, followed by a rapid drop, and finally decreasing gradually. It can be observed that as the diesel injection timing advances from 19° BTDC to 23° BTDC, the in-cylinder peak pressure increases significantly, indicating that

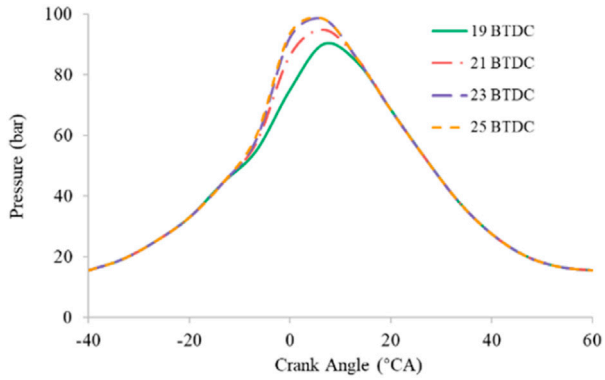

FIGURE 6
Cylinder pressure for various diesel pilot injection timings.

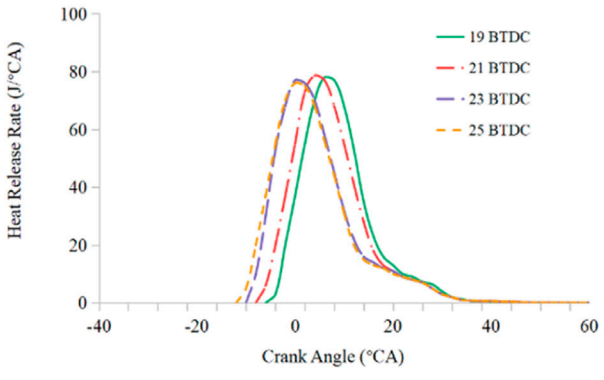

FIGURE 7
Cylinder heat release for various diesel pilot injection timings.

appropriately advancing the diesel injection timing helps increase the in-cylinder pressure. However, the change in cylinder pressure when advancing from 23° BTDC to 25° BTDC is relatively small. The corresponding maximum pressures (Pmax) are 97.8 bar and 98.6 bar, respectively. The pressure rise rates (dp/dθ) are 3.9 bar/°CA and 4.5 bar/°CA, respectively. The crank angles corresponding to their maximum pressures are 5.5° CA and 7.3° CA, respectively. When the pilot diesel injection timing was advanced from 19° BTDC to 25° BTDC, the ignition delay period was prolonged, and the combustion phase was retarded. This facilitates the formation of a more fuel-air mixture before the start of combustion, thereby promoting the generation of ignition centers (Tripathi et al., 2022; Zhou et al., 2019).

Figure 7 presents the variation characteristics of the heat release rate under each of the aforementioned operating conditions. As can be inferred from the curve trends, the crank angle at which the combustion process initiates is relatively earlier. However, it is noteworthy that as the pilot injection timing is advanced to an earlier angle, the peak heat release rate exhibits a slight decrease. Across all test operating conditions, regardless of how the pilot injection timing is set, the end position of the combustion process remains essentially consistent, all occurring at approximately 35° ATDC. A plausible explanation is that since natural gas exists in the cylinder in a premixed form, once the diesel flame ignites, its combustion mainly proceeds through turbulent flame propagation. However, under naturally aspirated conditions, the in-cylinder turbulent intensity is limited. As the piston moves downward, the in-cylinder volume increases rapidly, causing the turbulence to decay quickly, and the flame propagation speed decreases accordingly. In addition, natural gas combustion itself has a longer chemical reaction time scale (compared to diesel diffusion combustion). Especially in an environment without EGR dilution and with high oxygen concentration, although ignition is easy, flame propagation is still limited by mixture uniformity and turbulent intensity. Therefore, regardless of when diesel ignites, the time required for the complete combustion of natural gas is primarily determined by the in-cylinder flow field and thermodynamic environment, which remain relatively constant under the same speed and load, resulting in a tendency for the combustion end time to be consistent. In this experiment, although EGR or turbine regulation was not used, within the tested SOI range, the maximum pressure rise rate did not exceed the safety threshold, and the cylinder pressure signal did not show high-frequency oscillation characteristics, indicating that no obvious knocking occurred. By integrating the heat release rate curve, the heat release amounts corresponding to the timing from 19° BTDC to 25° BTDC are 1,208.1J, 1,256.3J, 1287J, and 1293J, respectively. This result indicates that although advancing the injection timing pushes the combustion phase into the higher temperature and pressure region around TDC, which should accelerate combustion, the pilot diesel fuel undergoes over-leaning due to an excessively long ignition delay, resulting in a reduced energy density of the ignition kernel. This weak kernel effect offsets the increased reaction rate brought about by the improved thermodynamic conditions, ultimately causing the combustion process to exhibit a unique translational shift characteristic, rather than the combustion duration shortening characteristic expected in traditional diesel engines.

Figure 8 shows the relationship between the burned mass fraction of diesel-compressed natural gas dual-fuel combustion and crank angle as a function of pilot injection timing under 75% engine load. The curve profiles under the four studied conditions are similar and can be divided into three main stages: a gradual increase first, followed by a sharp rise, and finally leveling off. The heat release start points for the injection timings of 23° BTDC and 25° BTDC are nearly identical. Additionally, as the pilot injection timing advances from 19° BTDC to 21° BTDC and further to 23° BTDC, the heat release start point also advances. Therefore, it can be concluded that a slight advance in pilot injection timing can improve the power output of the dual-fuel engine. However, studies have shown that the peak pressure rise rate (dp/dθ) caused by excessively early injection may exceed the fatigue limit of the engine cylinder block. In such cases, it is necessary to reduce the combustion rate by retarding the injection timing or adopting EGR (Sremec et al., 2017).

Figure 9 illustrates the variation of ignition delay for different pilot injection angles as the engine load increases. Ignition delay consists of two stages: physical processes and chemical processes. The physical processes include fuel injection, atomization, vaporization, and air-fuel mixing, while the chemical processes involve chemical reactions between fuel and air before combustion (Wei et al., 2024). In this

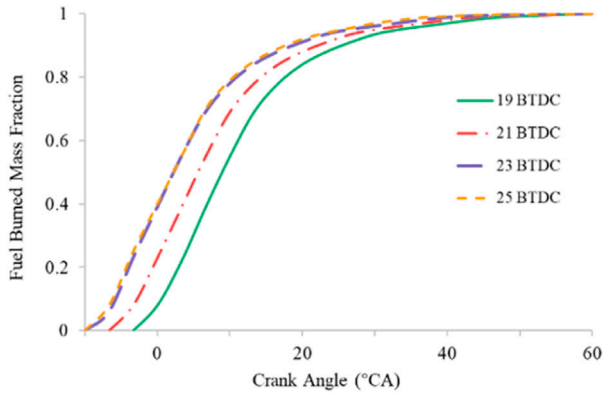

FIGURE 8
Burned mass fraction for various diesel pilot injection timings.

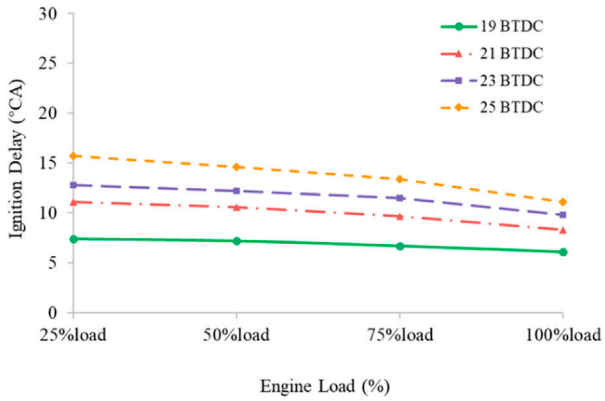

FIGURE 9
Ignition delay of various diesel pilot injection timings under different engine loads.

study, as the engine load increases, the ignition delay of dual-fuel combustion gradually shortens. It was observed that with the increase in engine load, the ignition delay of diesel-compressed natural gas dual-fuel combustion can be shortened by approximately 1.3–4.6 crank angle degrees by retarding the pilot injection timing. Furthermore, as the engine load increases, the maximum difference in ignition delay between different pilot diesel injection timings narrows. Experiments show that when the engine loads are 25%, 50%, 75%, and 100% respectively, and as the pilot diesel injection timing advances from 19° BTDC to 21° BTDC, 23°BTDC, and 25°BTDC, the maximum differences in ignition delay are 1.3, 2.8, 3.0, and 4.6 crank angle degrees, respectively.

Figure 10 shows the conditions of CA10, CA50, and CA90 under different fuel injection timings. It can be observed that as the fuel injection timing advances from 19°BTDC to 25°BTDC, the overall combustion process is advanced; however, the changes in combustion duration and combustion rate are relatively small. The combustion phase advances under all operating conditions, but the combustion duration only changes slightly. This is consistent with the fact that the position of the peak heat release in Figure 7 advances as the fuel injection advances, while the width of the heat release peak (i.e., the combustion duration) remains the same, indicating that the combustion process is "shifted as a whole" rather than "stretched or compressed". In the dual-fuel system, the combustion phase is adjustable, while the combustion duration remains stable, providing a solid foundation for the combustion control strategy.

2.3 Exhaust emissions

Figure 11 illustrates the variation in smoke opacity during NDDF combustion mode with respect to pilot injection timing under different loads. Smoke emissions are primarily associated with the pilot diesel fuel, as well as CNG, whose main component is methane, which does not produce particulate matter during combustion. It can be observed that, under the same injection timing, the smoke opacity of the diesel-CNG dual-fuel engine increases with increasing engine load, which is attributed to the decrease in air volumetric efficiency during combustion. It should be noted that the smoke opacity decreases as the pilot injection timing is advanced. The smoke opacity reached its greatest reduction when the fuel injection timing was 25°BTDC. Specifically, on the 100% load condition, the reduction reaches 4.2%. This is attributed to the advanced injection of the pilot fuel, which promotes the complete oxidation of soot into carbon dioxide, thereby reducing smoke emissions (Song et al., 2020).

Figure 12 illustrates the variation of NO_x emissions from the dual-fuel engine with the pilot injection timings under different engine loads. Under the investigated conditions, NO_x emissions increase with increasing load. NO_x emissions are relatively low in the 25%–75% load range and higher under 100% load conditions. This is because the engine temperature is lower at low loads, and the cooling effect of CNG intake also reduces the combustion temperature, thereby decreasing the formation of thermal NO_x. At high loads, the engine temperature is higher, turbulence in the combustion chamber is enhanced, and the flame propagation speed is accelerated (Abdelaal and Hegab, 2012; Papagiannakis et al., 2010; John Heywood, 2018).

When investigating the effect of varying the pilot injection timing on NO_x emissions, it is found that NO_x emissions reach their highest value at 25° BTDC and drop to their lowest value at 19° BTDC. It can be seen that NO_x emissions increase as the pilot injection timing is advanced. This is because advanced injection timing leads to advanced ignition, which raises the combustion temperature in the flame zone. A comparison with Figure 11 reveals that, under the same 100% load condition, the smoke emission is the highest and the NO_x emission is the lowest when the pilot injection timing is 19° BTDC. In contrast, the situation is opposite when the timing is advanced to 25° BTDC. Therefore, this trade-off relationship needs to be considered when optimizing emissions.

Figure 13 illustrates the variation in CO emissions from the dual-fuel engine with different injection timings at varying engine loads. Under low-load conditions, CO emissions are relatively high due to the reduced in-cylinder temperature. As the engine load increases, CO emissions generally show a decreasing trend because of the elevated temperature. With the advance of the pilot injection timing, CO emissions exhibit an overall increasing trend. When the injection timing is advanced to 25° BTDC, the in-cylinder pressure and temperature at the moment of diesel injection are lower compared

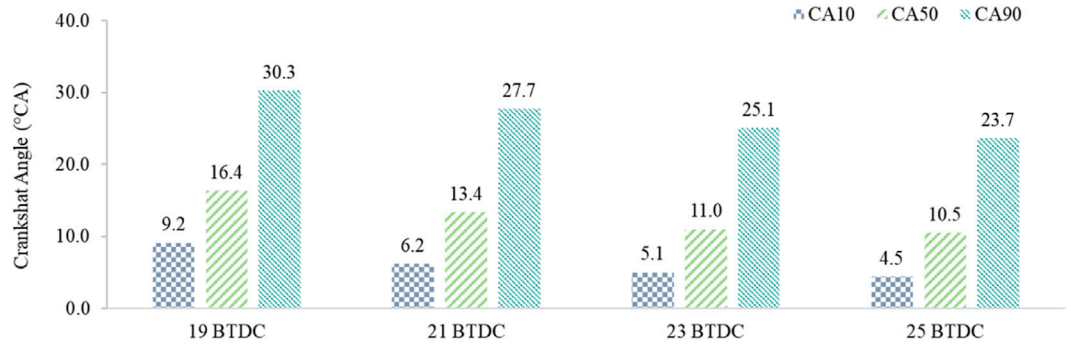

FIGURE 10
Combustion phases under different ignition timings.

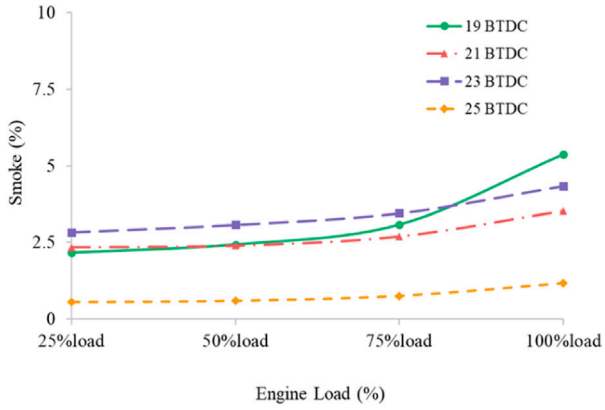

FIGURE 11
Smoke opacity of various diesel pilot injection timings under different engine loads.

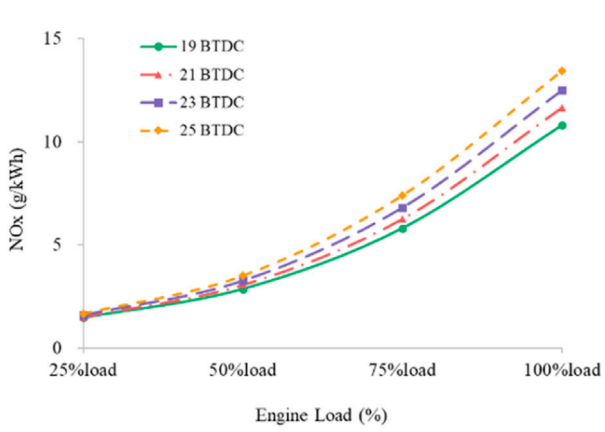

FIGURE 12
NO_x emissions of various diesel pilot injection timings under different engine loads.

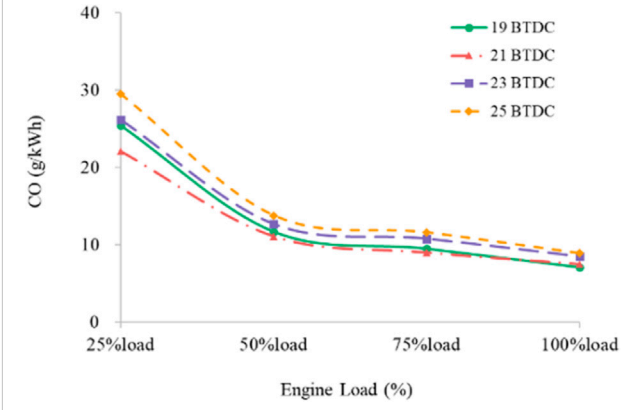

FIGURE 13
CO emissions of various diesel pilot injection timings under different engine loads.

to 19° BTDC. This results in a prolonged ignition delay for the pilot diesel, causing the fuel to over-lean with the surrounding air-CNG charge prior to ignition. This process creates regions of ultra-lean mixtures, leading to localized incomplete combustion (Yuvenda et al., 2019). Furthermore, during the early compression stroke, the larger cylinder volume facilitates the entrapment of unburned CNG-air mixture into the piston ring crevices (crevice volumes). Since the combustion process is primarily concentrated in the main chamber, the flame front fails to penetrate these crevices, leaving the trapped mixture unburned. These species are subsequently released as CO during the exhaust stroke. Based on the above, with the advancement of injection timing, these factors collectively led to an increase in CO emissions (Chintala, 2020).

Figure 14 shows that as the load increases from 25% to 75%, the specific CO2 emissions exhibit a significant downward trend, reaching their lowest point at 75% load. This is mainly attributed to the improvement in the BTE of the engine. Under medium and high loads, the proportion of mechanical friction losses and pumping losses in the total power consumption decreases, and the combustion conditions improve. However, under the 100% load condition, due to the reduction in the excess air ratio, the mixture becomes relatively richer, leading to a slight rebound in specific emissions. By comparing this phenomenon with the soot trends shown in Figure 11, it is evident that at the advanced injection timing of 25° BTDC, the higher in-cylinder temperature (confirmed by the high NOx content in

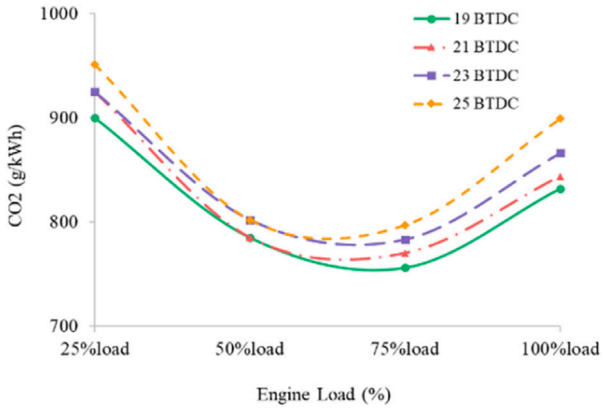

FIGURE 14
CO_2 emissions of various diesel pilot injection timings under different engine loads.

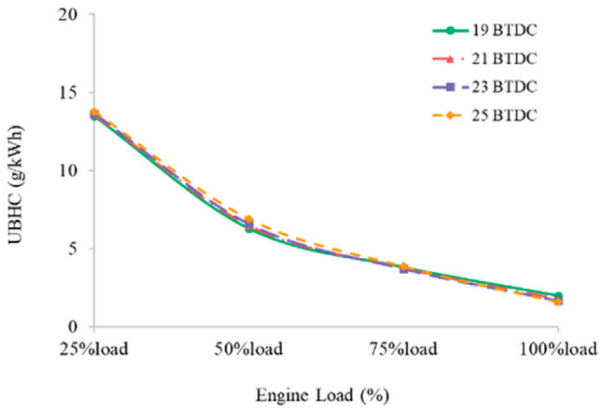

FIGURE 15
HC emissions of various diesel pilot injection timings under different engine loads.

Figure 12) promotes the complete oxidation of soot into carbon dioxide. Therefore, this high carbon conversion efficiency ultimately leads to an increase in the measured specific CO2 emissions.

Figure 15 presents the variation of unburned hydrocarbon (HC) emissions from the dual-fuel engine with the pilot injection timings under different engine loads. It can be observed that HC emissions decrease with the increase in engine load under all operating conditions. Some studies have proposed that the formation of HC is directly related to excessively low combustion temperature, overly lean mixture, or the wall quenching effect. Diesel injection timing regulates the amount of HC generated by influencing the number of ignition centers and the flame propagation path. Under low-load conditions, appropriately advancing the injection creates multiple ignition centers, which can cover a wider range of the natural gas mixture, reduce local overly lean regions, and significantly lower HC emissions (Yuvenda et al., 2019). However, excessively advanced injection may cause a rebound in HC emissions due to the condensation of diesel in low-temperature regions, which is associated with unburned diesel in the piston top crevices (Willems et al., 2021). Nevertheless, no obvious regularity in HC emissions was observed in relation to variation in pilot injection timing in this study. According to Table 2, the hydrocarbon analyzer has a detection range of 0–10,000 ppm, an accuracy of ±30 ppm, and an uncertainty of 3.35%. The concentration range of unburned HC measured under different operating conditions is approximately between 500ppm and 1500ppm. Relatively high uncertainty and large precision errors indicate that small changes in hydrocarbon concentrations may fall within the noise range of the instrument, which makes it difficult to detect subtle trends.

Figure 16 shows the trade-off between NO_x emissions and smoke opacity under different pilot injection timings and load conditions. A clear inverse relationship can be observed, where reducing smoke opacity generally leads to an increase in NO_x, and an increase in smoke opacity is accompanied by a decrease in NO_x. Under all tested conditions, the pilot injection timing of 25° BTDC consistently achieves the lowest smoke levels across all loads, indicating that the mixing effect has been improved and combustion is more complete. However, due to the increase in peak temperature and earlier heat release, this can also lead to higher nitrogen oxide emissions, especially

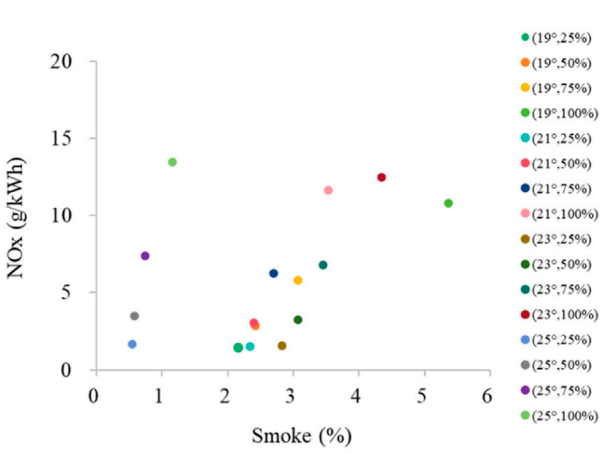

FIGURE 16
Trade-off between NO_x and Smoke opacity.

under high loads. In contrast, the injection timing 19°BTDC generates higher smoke density, but NO_x emissions are relatively lower. This indicates that the combustion is shifting towards a diffusion-dominated regime, reducing the generation of thermogenic NO_x. These results indicate that by optimizing injection timing and load, both emissions can be reduced simultaneously, thereby achieving the best performance of the engine.

3 Conclusion

In this study, the comprehensive influence mechanism of diesel pilot injection timing on the performance of NDDF engines was elucidated through experiments conducted under full-load conditions. The main conclusions are as follows.

1. Identification of the full-load boundary of efficiency deterioration: within the load range of 25%–75%, advancing the pilot injection timing generally improves the BTE.

However, there is an efficiency inflection point at 100% load: advancing the pilot injection to 25° BTDC will lead to a decrease in BTE. This indicates that under high-load conditions, the pilot injection strategy needs to achieve a balance between complete combustion and the negative compression work resulting from pilot injection.

2. The discovery of the combustion phase decoupling phenomenon: experiments show that as the injection timing advances, the heat release rate curve shows a translational shift rather than a compressed characteristic. This is a characteristic of dual-fuel engines: the longer ignition delay leads to over-leaning of the diesel spray, creating weak ignition cores, thereby limiting the initial flame propagation speed. This effect persists even with an optimized pilot diesel amount, which counteracts the reaction rate gains typically provided by the high-temperature environment near TDC.
3. Determinations of emission trade-off and control strategies: advancing injection timing proved effective for reducing soot emissions, achieving a significant reduction at 100% load, but at the cost of a significant increase in NO_x emissions. The increase in NO_x at full load is further driven by the elevated in-cylinder temperatures and the increased proportion of diesel diffusion combustion employed to prevent knock. Additionally, the observed increase in CO emissions with advanced timing confirms that excessively early injection leads to localized over-lean mixtures.

In conclusion, for the optimization of dual-fuel engines, a careful consideration of the negative work boundary at full load, the knock-limit constraints, and the ignition kernel formation is essential to achieve the optimal trade-off between efficiency and emissions.

Data availability statement

The original contributions presented in the study are included in the article/supplementary material, further inquiries can be directed to the corresponding author.

Author contributions

YW: Writing – review and editing, Writing – original draft. TQ: Writing – review and editing, Supervision.

Funding

The author(s) declared that financial support was not received for this work and/or its publication.

Conflict of interest

The author(s) declared that this work was conducted in the absence of any commercial or financial relationships that could be construed as a potential conflict of interest.

Generative AI statement

The author(s) declared that generative AI was not used in the creation of this manuscript.

Any alternative text (alt text) provided alongside figures in this article has been generated by Frontiers with the support of artificial intelligence and reasonable efforts have been made to ensure accuracy, including review by the authors wherever possible. If you identify any issues, please contact us.

Publisher's note

References

Abdelaal, M. M., and Hegab, A. H. (2012). Combustion and emission characteristics of a natural gas-fueled diesel engine with EGR. *Energy Convers. Manag.* 64, 301–312. doi:10.1016/j.enconman.2012.05.021

Akbarian, E., Najafi, B., Jafari, M., Ardabili, S. F., Shamshirband, S., and Chau, K. W. (2018). Experimental and computational fluid dynamics-based numerical simulation of using natural gas in a dual-fueled diesel engine. *Eng. Appl. Comput. Fluid Mech.* 12, 517–534. doi:10.1080/19942060.2018.1472670

Chintala, V. (2020). Influence of flame quenching and crevice gas on hydrocarbon emission formation in an enriched biogas dual-fuel engine – an experimental and theoretical investigation. *Fuel* 277, 118084. doi:10.1016/j.fuel.2020.118084

Coleman, W., Glenn Steck, W., and Wiley, J. (1989). *Experimentation and uncertainty analysis for engineers*, 443. Prentice-Hall, Inc.

Dai, X., Singh, S., Krishnan, S. R., and Srinivasan, K. K. (2020). Numerical study of combustion characteristics and emissions of a diesel–methane dual-fuel engine for a wide range of injection timings. *Int. J. Engine Res.* 21, 781–793. doi:10.1177/1468087418783637

Dimitriou, P., Tsujimura, T., Kojima, H., Aoyagi, K., Kurimoto, N., and Nishijima, Y. (2020). Experimental and simulation analysis of natural gas-diesel combustion in dual-fuel engines. *Front. Mech. Eng.* 6, 543808. doi:10.3389/FMECH.2020.543808

Guo, H., Liko, B., Habash, B., D'Arcy, R. C., and Song, X. (2018a). Injector tip temperature and combustion performance of a natural gas-diesel dual fuel engine at medium and high load conditions. *Aging Med.* 1: 75–95. American Society of Mechanical Engineers. doi:10.1115/ICEF2018-9664

Guo, H., Liko, B., Luque, L., and Littlejohns, J. (2018b). Combustion performance and unburned hydrocarbon emissions of a natural gas–diesel dual fuel engine at a low load condition. *J. Eng. Gas. Turbine Power* 140, 112801. doi:10.1115/1.4039758

Jamrozik, A., Tutak, W., and Grab-Rogaliński, K. (2019). An experimental study on the performance and emission of the diesel/CNG dual-fuel combustion mode in a stationary CI engine. *Energies (Basel)* 12, 3857. doi:10.3390/en12203857

John Heywood - Internal combustion engine fundamentals-McGraw-Hill Education (2018).

Katrašnik, T., Trenc, F., and Opresnik, S. R. (2006). A new criterion to determine the start of combustion in diesel engines. *J. Eng. Gas. Turbine Power* 128, 928–933. doi:10.1115/1.2179471

Liu, J., Yang, F., Wang, H., Ouyang, M., and Hao, S. (2013). Effects of pilot fuel quantity on the emissions characteristics of a CNG/diesel dual fuel engine with optimized pilot injection timing. *Appl. Energy* 110, 201–206. doi:10.1016/j.apenergy.2013.03.024

López, J. M., Gómez, Á., Aparicio, F., and Fco, J. S. (2009). Comparison of GHG emissions from diesel, biodiesel and natural gas refuse trucks of the city of Madrid. *Appl. Energy* 86, 610–615. doi:10.1016/j.apenergy.2008.08.018

Namasivayam, A. M., Korakianitis, T., Crookes, R. J., Bob-Manuel, K. D. H., and Olsen, J. (2010). Biodiesel, emulsified biodiesel and dimethyl ether as pilot fuels for natural gas fuelled engines. *Appl. Energy* 87, 769–778. doi:10.1016/j.apenergy.2009.09.014

Pham, V. C., Choi, J.-H., Rho, B.-S., Kim, J.-S., Park, K., Park, S.-K., et al. (2021). A numerical study on the combustion process and emission characteristics of a natural gas-diesel dual-fuel marine engine at full load. *Energies (Basel)* 14, 1342. doi:10.3390/en14051342

Panoutsou, C., Germer, S., Karka, P., Papadokostantakis, S., Kroyan, Y., Wojcieszyk, M., et al. (2021). Advanced biofuels to decarbonise European transport by 2030: markets, challenges, and policies that impact their successful market uptake. *Energy Strategy Rev.* 34, 100633. doi:10.1016/j.esr.2021.100633

Papagiannakis, R. G., Rakopoulos, C. D., Hountalas, D. T., and Rakopoulos, D. C. (2010). Emission characteristics of high speed, dual fuel, compression ignition engine operating in a wide range of natural gas/diesel fuel proportions. *Fuel* 89, 1397–1406. doi:10.1016/j.fuel.2009.11.001

Ryu, K. (2013). Effects of pilot injection timing on the combustion and emissions characteristics in a diesel engine using biodiesel-CNG dual fuel. *Appl. Energy* 111, 721–730. doi:10.1016/j.apenergy.2013.05.046

Song, J., Feng, Z., Lv, J., and Zhang, H. (2020). Experimental study on combustion and performance of a natural gas-diesel dual-fuel engine at different pilot diesel injection timing. *J. Therm. Sci. Eng. Appl.* 12, 051013. doi:10.1115/1.4046011

Sremec, M., Taritaš, I., Sjerić, M., and Kozarac, D. (2017). Numerical investigation of injection timing influence on fuel slip and influence of compression ratio on knock occurrence in conventional dual fuel engine. *J. Sustain. Dev. Energy, Water Environ. Syst.* 5, 518–532. doi:10.13044/j.sdewes.d5.0163

Tripathi, G., and Dhar, A. (2022). Performance, emissions, and combustion characteristics of methane-diesel dual-fuel engines: a review. *Front. Therm. Eng.* 2, 870077. doi:10.3389/fther.2022.870077

Tripathi, G., Sharma, P., and Dhar, A. (2022). Computational study of diesel injection strategies for methane-diesel dual fuel engine. *Clean. Eng. Technol.* 6, 100393. doi:10.1016/j.clet.2021.100393

Wang, Z., Zhao, Z., Wang, D., Tan, M., Han, Y., Liu, Z., et al. (2016). Impact of pilot diesel ignition mode on combustion and emissions characteristics of a diesel/natural gas dual fuel heavy-duty engine. *Fuel* 167, 248–256. doi:10.1016/j.fuel.2015.11.077

Wang, Y., and Wright, L. A. (2021). A comparative review of alternative fuels for the maritime sector: economic, technology, and policy challenges for clean energy implementation. *World* 2, 456–481. doi:10.3390/world2040029

Wei, C., Chen, X. X., Chen, L., Li, P., and Liu, M. (2024). Effects of pilot oil injection timing on combustion, covariance and knocking of a natural gas-diesel duel-fuel low-speed engine. *Pol. Marit. Res.* 31, 69–75. doi:10.2478/pomr-2024-0051

Willems, R., Willems, F., Deen, N., and Somers, B. (2021). Heat release rate shaping for optimal gross indicated efficiency in a heavy-duty RCCI engine fueled with E85 and diesel. *Fuel* 288, 119656. doi:10.1016/j.fuel.2020.119656

Yousefi, A., Birouk, M., and Guo, H. (2020). On the variation of the effect of natural gas fraction on dual-fuel combustion of diesel engine under low-to-high load conditions. *Front. Mech. Eng.* 6, 555136. doi:10.3389/FMECH.2020.555136

Yuvenda, D., Sudarmanta, B., Wahjudi, A., and da, S. J. (2019). Characterization of engine performance, combustion process and emission of Diesel/CNG dual fuel engines with pilot injection timing variation at low load. *IOP Conf. Ser. Mater Sci. Eng.* 588, 012005. doi:10.1088/1757-899X/588/1/012005

Zhang, X., Gao, J., Fan, D., Yang, Q., Han, F., and Yu, H. (2024). Impact of pilot diesel injection timing on performance and emission characteristics of marine natural gas/diesel dual-fuel engine. *Sci. Rep.* 14, 10713. doi:10.1038/s41598-024-61672-5

Zhou, H., Zhao, H.-W., Huang, Y.-P., Wei, J.-H., and Peng, Y.-H. (2019). Effects of injection timing on combustion and emission performance of dual-fuel diesel engine under low to medium load conditions. *Energies (Basel)* 12, 2349. doi:10.3390/en12122349